

Ion Beam Assisted Deposition of $Ti_{50}Al_{50}N$

P. Aliotta and J. Krzanowski, University of New Hampshire, Durham, NH

ABSTRACT

The ion beam assisted sputter deposition (IBSD) technique has been used to deposit TiAlN thin films with the goal of controlling grain structure and thereby optimizing hardness and wear resistance. In the IBSD method the films are deposited using magnetron sputter sources along with a simultaneous argon ion bombardment from an ion gun. The effects of ion bombardment were examined under both acute and oblique angle deposition. The temperature during deposition was 450°C and the substrate bias was constant at -50V for all depositions. The films were examined using x-ray diffraction, nano-indentation hardness testing, and atomic force microscopy. For substrates that were stationary during deposition, higher degrees of ion bombardment resulted in grains forming an oblique angle to the substrate. However, for samples rotated during deposition, columnar grains formed normal to the substrate regardless of ion beam flux. The flux of incident ions helped improve the hardness with hardness levels of up to 37 GPa obtained, and also reduce the concentration of voids in the film. X-ray diffraction pole figures showed that the orientation of the grains could be altered using the ion beam assisted process.

INTRODUCTION

$Ti_{1-x}Al_xN$ films have been long studied for their use as a wear resistant coating in high performance machining due to the film's hardness and superior oxidation resistance [1-3]. When compared to conventional TiN coatings, TiAlN offers superior performance as it allows for higher cutting speeds and undergoes reduced wear over equal cutting distances [3]. TiAlN films have been most commonly deposited by PVD methods which causes a columnar micro structure growth that affects the mechanical [2-10], optical [11], and electrical properties [12] of grown films. Methods for controlling grain evolution include varying sputtering condition [2-3, 8-10], including a negative substrate bias [4-5], and controlling the deposition angle of the films [6, 13].

$Ti_{1-x}Al_xN$ itself is a metastable material and for sputtered films it was found that for $x < 0.53$ the films are single phase with B1-NaCl structure where larger values of x result in a two phase film with B1-NaCl AlN depleted grains and wurtzite- structure AlN rich grains [13]. It was also shown that the formation of wurtzite structured AlN grains resulted in a reduction in average grain size and increase in the intergranular void density of the films, which is undesirable for films when high hardness is a primary requirement.

This paper discusses research on the effects of varying ion irradiation rates and ion energy levels on the growth of TiAlN thin films. Ion irradiation is carried out using an end-hall ion source. During deposition the substrates were either stationary or rotated and the incident angles of the ions and sputtered metal atoms were also varied. Since the discharge current of an end-hall ion source is controlled by the anode voltage and gas flow rate to the gun, both parameters were varied independently as the anode voltage controls the ion energy and the gas flow rate affects the chamber pressure and thus the film growth. Films were evaluated using x-ray diffraction, atomic force microscopy (AFM) and nanoindentation for film hardness.

EXPERIMENTAL

$Ti_{1-x}Al_xN$ films were deposited by magnetron sputtering from a single $Ti_{50}Al_{50}$ source in a $Ar+N_2$ mixture. Sputtering took place in an AJA ATC 2000-f system which was pumped to a base pressure $\sim 10^{-7}$ Torr. All films were deposited on Si (100) and prior to TiAlN deposition ~ 50 nm of TiAl was deposited to improve adhesion. The Si (100) was ion etched prior to deposition to remove any oxide layer impurities and the target was sputter cleaned with the shutter closed prior to deposition.

Sputtering took place under the following constant conditions: a constant gas flow of 12.5 sccm Ar and 3.5 sccm N_2 and sputter gun power 7.72 W/cm². Substrate temperature was 450°C

<http://dx.doi.org/10.14332/svc13.proc.1101>

and was left to equalize the temperature for one hour prior to beginning deposition. A -50V bias was placed on the substrate and the bias current was measured to determine the current density ratio. Rotated samples were rotated at a speed of 50 rpm. Final film thicknesses ranged from 0.9 μm to 1.5 μm , which was measured by step profilometry. The amount of film sputtered off during deposition due to the increased use of the ion gun was accounted when determining film thicknesses.

The ions were generated by a Veeco End-Hall Mark II+ ion source. The discharge current of an End-Hall source was controlled by the gas flow, which was varied from 10-20 sccm independently of the gas flow to the sputter gun, and the anode voltage, which was varied from 60 V-120V. As varying the gas flow affects the chamber pressure and nitrogen concentration while the anode voltage controls the ion energy, the two parameters were varied independently with the gas flow being held constant at 17 sccm with the anode voltage varied and the anode voltage held constant at 85 V while the gas flow was varied.

X-Ray diffraction and pole figures were gathered in a Bruker AXS area detection system. AFM measurements and nanoindentation was done using a Digital Instruments Dimension 3000 scanning probe microscope with a Hysitron Triboscope Nano-mechanical Test system. Hardness values were collected by taking indentations of ~ 100 nm and having the computer calculate values from load vs. displacement plots within the Triboscope software. Tool wear tests were also conducted depositing placing films on Sandvik SPG-422 carbide inserts and measuring flank wear while cutting 1040 steel. The cutting speed was 180 m/min with a feed rate of 0.11 mm/rev and depth of cut of 0.25 mm.

RESULTS AND DISCUSSION:

XRD scans

XRD scans of samples with films deposited 20° from normal with constant gas flow of 17 sccm Ar to the ion gun are shown in Figure 1a, for stationary samples, and 1b for rotated samples. For the figures, j_i/j_m is the ion to metal current density ratio.

In each plot for $j_i/j_m = 0$ the scan shows a single phase B1 NaCl-type structure, however as the current density increases a shift in the peaks indicates an increasing amount of stress in the films caused by the increasing rate of ion bombardment. The (111) peak is of considerable interest as it has been shown that upon increasing the Al content in the film the (111) peak splits into two parts [2]. This precipitation of the AlN wurtzite structure can be also caused by annealing at high temperature [13]. For stationary depositions peak splitting indicates that stress and ion bombardment on the films causes AlN precipitation, however this can be suppressed as the rate of ion incidence increases past $j_i/j_m = 1$ indicating that the ability of an ion source to cause AlN precipitation is not simply a function of individual ion energy or the ratio of ions to metal atoms incident on the sample.

Figure 2a,b show XRD scans for depositions 40° from normal at constant gas flow of 17 sccm with Figure 3a being the scans of stationary samples and Figure 3b being scans of rotated samples. These scans, comparing rotated to stationary samples show peak splitting occurring for values of $.5 < j_i/j_m < 1$ with a larger amount of AlN precipitation taking place in the stationary sample.

Pole figures

Pole figure analysis was also performed with Figure 3 showing the (111) and (200) poles for stationary samples and Figure 4 showing the (111) and (200) poles for rotated samples.

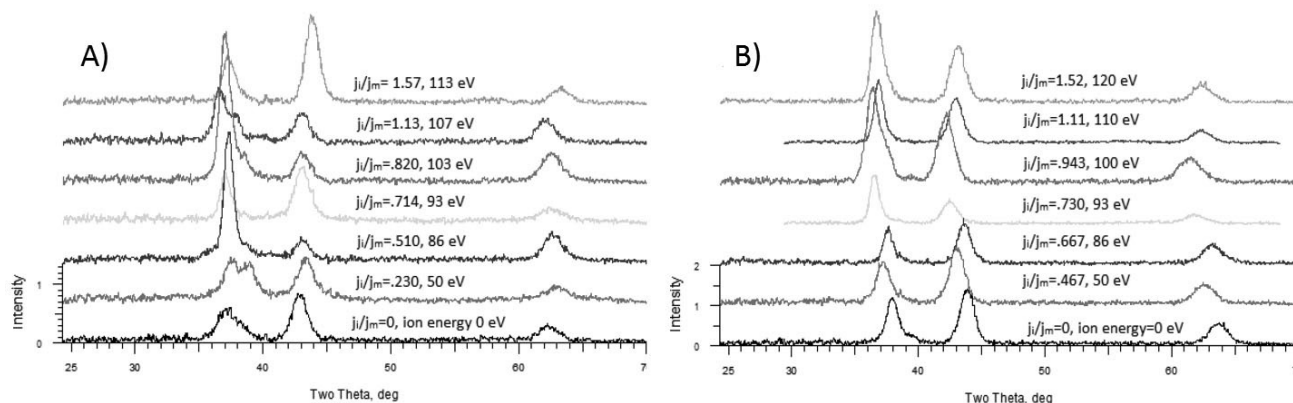


Figure 1: Room temperature XRD scans of ion beam assisted $\text{Ti}_{30}\text{Al}_{50}\text{N}$ samples deposited at 450° and 20° from normal, while A) stationary and B) rotated. Ion to metal current ratios are listed as j_i/j_m and mean ion energies are given in eV. Gas flow to the ion gun was 17 sccm Ar for all runs.

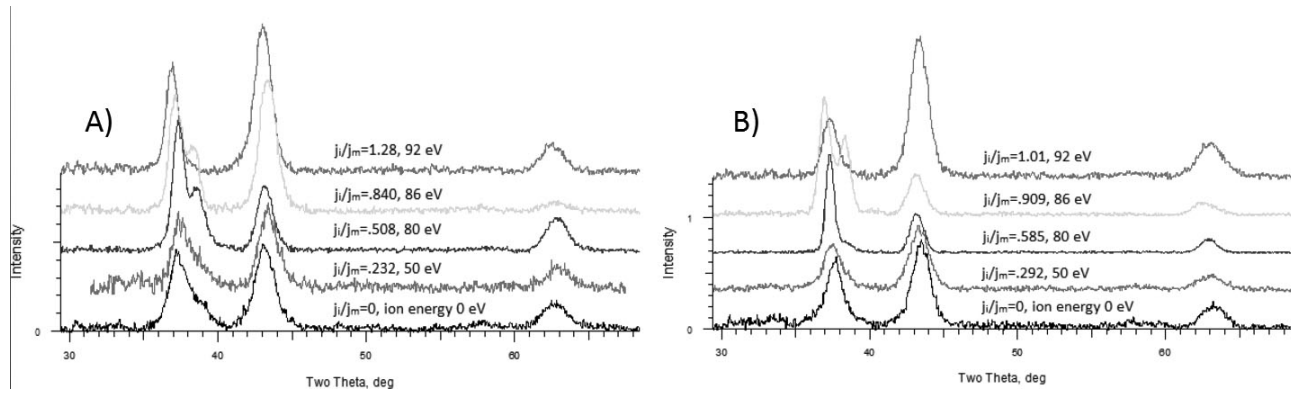


Figure 2: Room temperature XRD scans of ion beam assisted $Ti_{50}Al_{50}N$ samples deposited at 45° and 40° from normal, while A) stationary and B) rotated. Ion to metal current ratios are listed as j_i/j_m and mean ion energies are given in eV. Gas flow to the ion gun was 17 sccm Ar for all runs.

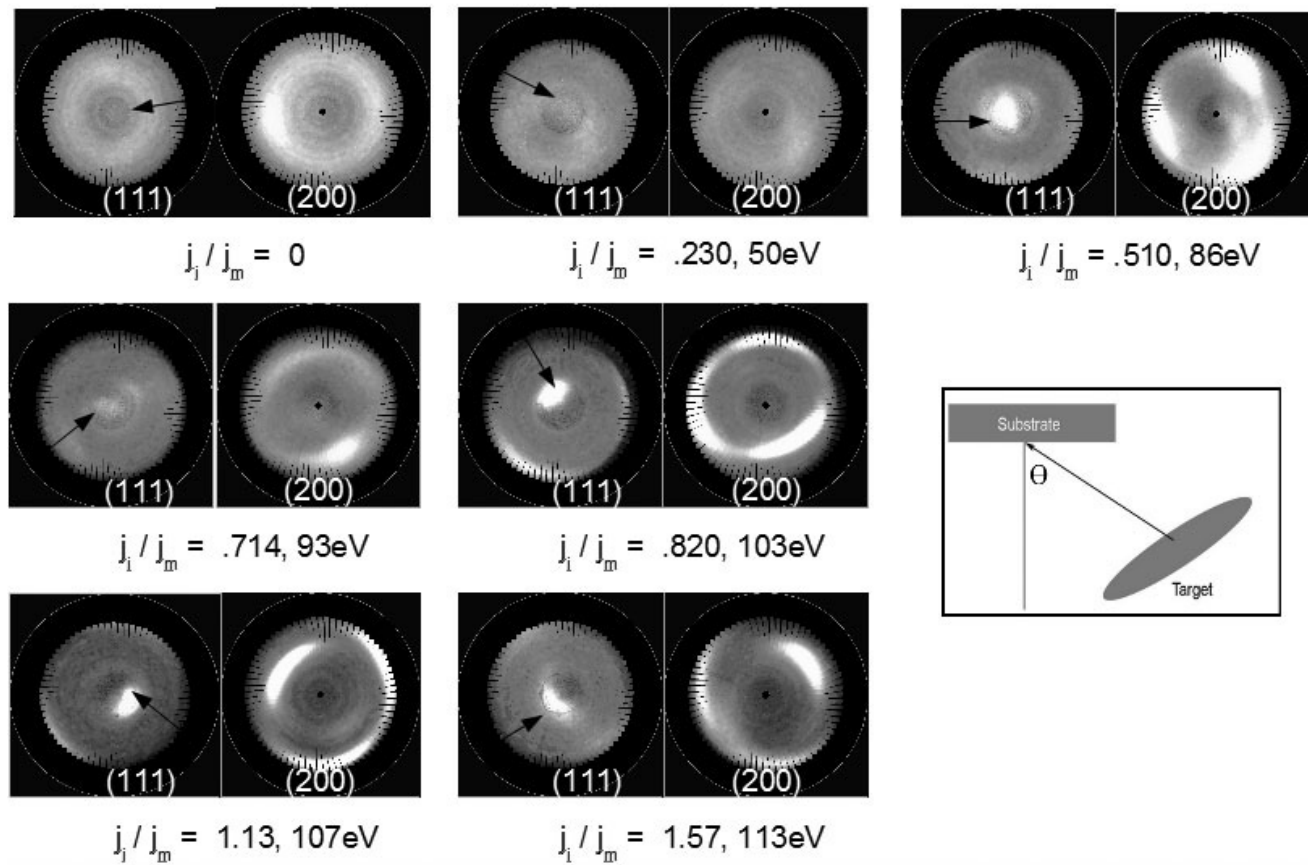


Figure 3: (111) and (200) Pole figures for ion beam assisted $Ti_{50}Al_{50}N$ deposited at 20° from normal while stationary. Ion to metal current ratios are listed as j_i/j_m and mean ion energies are given in eV. Gas flow to the ion gun was 17 sccm Ar for all runs.

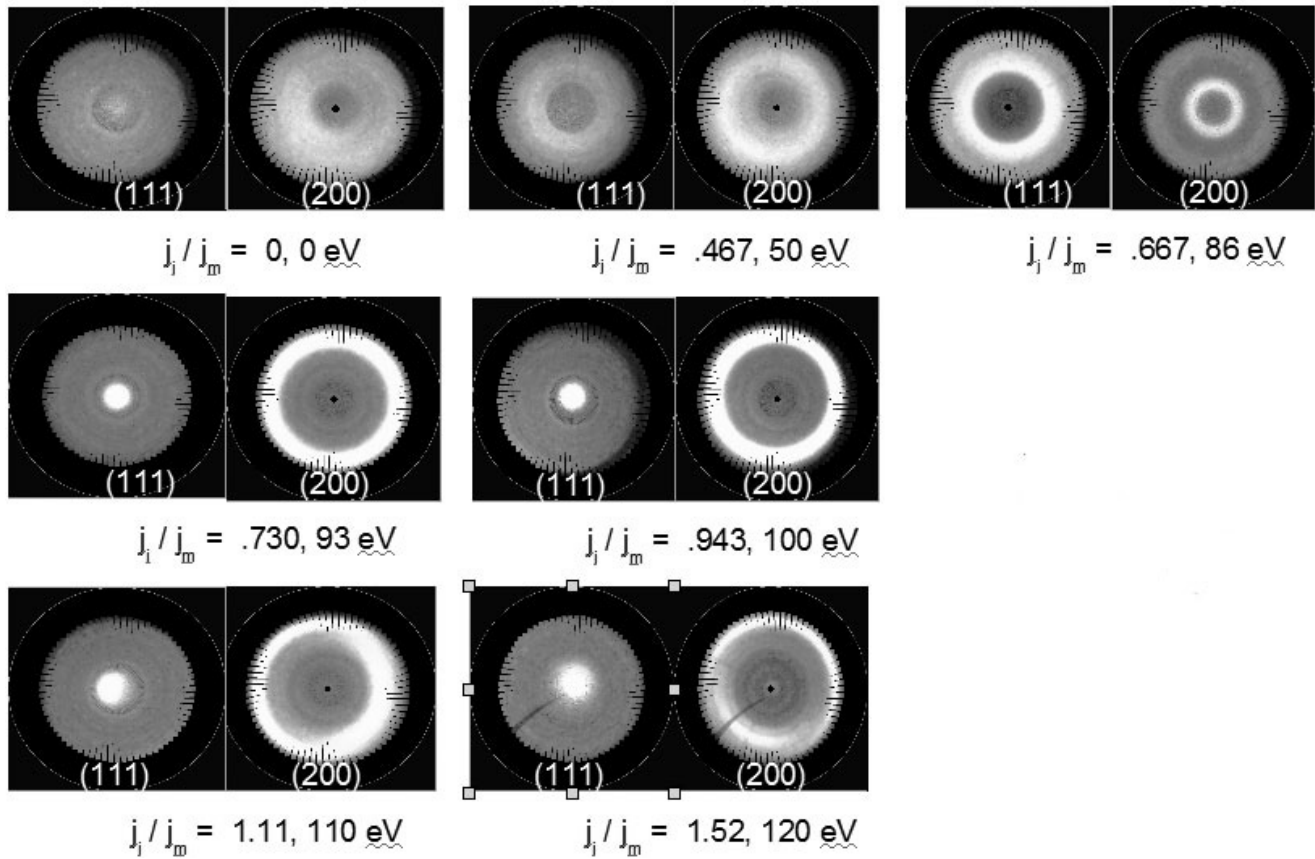


Figure 4: (111) and (200) Pole figures for ion beam assisted $Ti_{50}Al_{50}N$ deposited at 40° from normal while rotated. Ion to metal current ratios are listed as j_i/j_m and mean ion energies are given in eV. Gas flow to the ion gun was 17 sccm Ar for all runs.

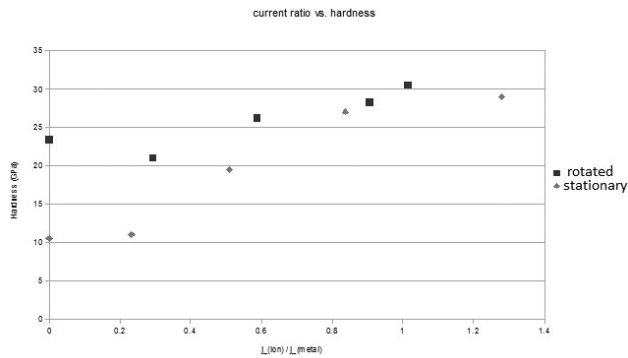


Figure 5: Hardness as a function of ion to metal current density ratio, as measured by nanoindentation, for rotated and stationary $TiAlN$ samples deposited at 40° from normal

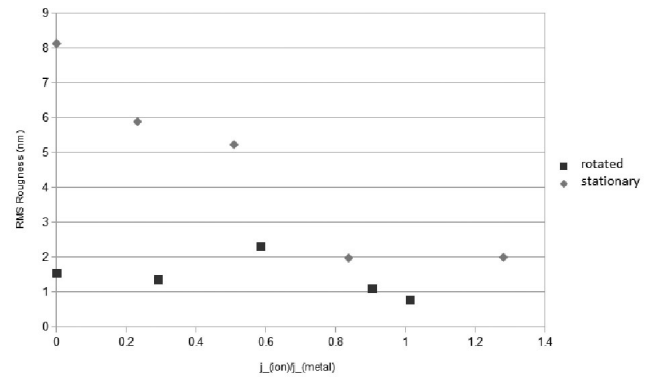


Figure 6: RMS roughness as a function of ion to metal current density ratio, as measured by nanoindentation, for rotated and stationary $TiAlN$ samples deposited at 40° from normal

Rotated samples show (111) planes parallel to the substrate surface and the (200) planes $\sim 57^\circ$ from normal indicating that these planes correspond to the same grains as the (111) planes. Stationary samples show a high degree of preferred alignment of the grains with the (111) planes tilted slightly towards the deposition source and the (200) planes showing alignment corresponding to the direction of deposition.

AFM results

Nanoindentation measurements were made and surface roughness was determined for samples deposited at 40° to normal, both rotated and stationary. Results of nanoindentation are shown in Figure 5, the initial hardness of the stationary samples is quite low for TiAlN at 10.5 GPa, however as the ion to metal current density ratio increases both the stationary and rotated samples increase in hardness. Surface roughness calculations as shown in Figure 6 were also made with the RMS roughness decreasing for both stationary and rotated samples as the ion to metal current density ratio increases.

CONCLUSION

Ti₅₀Al₅₀N has been deposited on Si (100) at 450° using ion beam assisted magnetron sputtering from a Ti₅₀Al₅₀ target. The discharge current from an end-hall ion source is controlled by adjusting the anode voltage and gas flow to the ion source, both parameters were independently adjusted to determine their effect on film growth. XRD investigations on the effects of ion beam bombardment of TiAlN films during magnetron sputtering has shown that increasing the discharge current/ ion energy has caused (111) peak splitting in TiAlN which is indicative of phase separation and the precipitation of wurtzite structured AlN, however at large ion currents the NaCl structure returns. The increasing ion currents also cause strain in the films during growth. AFM and nanoindentation measurements have also shown that increasing ion currents/ energies cause decreased surface roughness and increased hardness in deposited films as measured by nanoindentation. These films also showed a marked improvement in practical machining tests for wear resistance.

ACKNOWLEDGEMENTS

The authors are grateful for the support of the US National Science Foundation under grant # CMMI/MCME-1031052.

REFERENCES

1. W.-D. Münz, "Titanium Aluminum Nitride Films: A new alternative to TiN coatings" *J. Vac. Sci. Technol.*, A4, (1986) 2712.
2. J. Musil, H. Hruby, "Superhard nanocomposite Ti_{1-x}Al_xN films prepared by magnetron sputtering" *Thin Solid Films* 365, (2000), 104-109.
[http://dx.doi.org/10.1016/S0040-6090\(00\)00653-2](http://dx.doi.org/10.1016/S0040-6090(00)00653-2)
3. H.C. Barshilia, K. Yogesh, K.S. Rajam, "Deposition of TiAlN coatings using reactive bipolar-pulsed direct current unbalanced magnetron sputtering", *Vacuum* 83, (2008), 427.
<http://dx.doi.org/10.1016/j.vacuum.2008.04.075>
4. C.-S. Chen, C.-P. Liu, H.-G. Yang, and C.-Y. A. Tsao, "Influence of substrate bias on practical adhesion, toughness, and roughness of reactive dc-sputtered zirconium nitride films", *J. Vac. Sci. & Tech. A* (22), (2004) 2041.
5. B.-Y. Shew, J.-L. Huang, D.-F. Lii, "Effects of r.f. Bias and nitrogen flow rates on the reactive sputtering of TiAlN films" *Thin Solid Films* 293, (1997) 212-219.
[http://dx.doi.org/10.1016/S0040-6090\(96\)09038-4](http://dx.doi.org/10.1016/S0040-6090(96)09038-4)
6. A.R. Shetty, A. Karimi, M. Cantoni, "Effect of deposition angle on the structure and properties of pulsed-DC magnetron sputtered TiAlN films", *Thin Solid Films* 519, (2011), 4262-4270.
<http://dx.doi.org/10.1016/j.tsf.2011.02.090>
7. M. Pinkas, J. Pelleg, M.P. Dariel, "Structural analysis of (Ti_{1-x}Al_x)N graded coatings deposited by reactive magnetron sputtering", *Thin Solid Films* 355-356, (1999), 380-384.
[http://dx.doi.org/10.1016/S0040-6090\(99\)00667-7](http://dx.doi.org/10.1016/S0040-6090(99)00667-7)
8. J.C. Oliveira, A. Manaia, A. Cavaleiro, "Hard Amorphous Ti-Al-N coatings deposited by sputtering" *Thin Solid Films* 516, (2008), 5032-5038.
<http://dx.doi.org/10.1016/j.tsf.2008.02.006>
9. K. Bobzin, E. Lugscheider, M. Maes, P. Immich, S. Bolz, "Grain size evaluation of pulsed TiAlN nanocomposite coatings for cutting tools", *Thin Solid Films* 515, (2007) 3681-3684.
<http://dx.doi.org/10.1016/j.tsf.2006.11.002>
10. A. Buranawong, N. Witit-anun, S. Chaiyakun, A. Po-kaipisit, P. Limsuwan, "The effect of titanium current on structure and hardness of aluminum titanium nitride deposited by reactive unbalanced magnetron co-sputtering" *Thin Solid Films* 519, (2011), 4963-4968.
<http://dx.doi.org/10.1016/j.tsf.2011.01.062>
11. H.C. Barshilia, C. Harish, N. Selvakumar, G. Vignesh, and A. Biswas, "Optical Properties and thermal stability of pulsed-sputter-deposited Al_xO_y/Al/Al_xO_y multilayer absorber coatings" *Sol. Energy Materials & Sol. Cells* 93 (3), (2009), 315.
<http://dx.doi.org/10.1016/j.solmat.2008.11.005>

-
12. S.-Y. Lee, S.-C. Wang, J.-S. Chen, J.-L. Huang, "Effects of deposition and post annealing conditions on electrical properties and thermal stability of TiAlN films by ion beam sputter deposition", *Thin Solid Films* 515, (2006) 1069.
<http://dx.doi.org/10.1016/j.tsf.2006.07.172>
 13. U. Wahlstrom, L. Hultman, J.-E. Sundgren, "Crystal growth and microstructure of polycrystalline $Ti_{1-x}Al_xN$ alloy films deposited by ultra-high-vacuum dual target magnetron sputtering", *Thin Solid Films* 235, (1993), 62-70.
[http://dx.doi.org/10.1016/0040-6090\(93\)90244-J](http://dx.doi.org/10.1016/0040-6090(93)90244-J)